geosciences

MDPI

Article

Seismic and Rainfall Induced Displacements of an Existing Landslide: Findings from the Continuous Monitoring

Paolo Ruggeri *, Viviene M. E. Fruzzetti, Antonio Ferretti and Giuseppe Scarpelli *

Department of Materials, Environmental Sciences and Urban Planning-Università Politecnica delle Marche, 60131 Ancona, Italy; v.m.e.fruzzetti@staff.univpm.it (V.M.E.F.); a.ferretti@pm.univpm.it (A.F.)

* Correspondence: p.ruggeri@staff.univpm.it (P.R.); g.scarpelli@staff.univpm.it (G.S.)

Received: 21 January 2020; Accepted: 24 February 2020; Published: 27 February 2020

Abstract: "La Sorbella" is a deep-seated existing landslide in a Miocene clayey formation located in central Italy. Given the interaction with a national road, this landslide has been monitored for a long time with inclinometers and hydraulic piezometers. Recently, the monitoring system was implemented by adding pressure transducers in the Casagrande cells and by equipping the old inclinometers with in-place probes, to allow a remote reading of the instruments and data recording. This system allowed to identify that the very small average rate of movement observed over one year (1.0–1.5 cm/year) is the sum of small single sliding processes, strictly linked to the sequence of rainfall events. Moreover, data recorded by in-place inclinometer probes detected the response of the landslide to the seismic sequence of 2016 occurring in central Italy. Such in situ measurements during earthquakes, indeed rarely available in the scientific literature, allowed an assessment of the critical acceleration of the sliding mass by means of a back-analysis. The possibility to distinguish the difference between seismic and rainfall induced displacements of the slope underlines the potential of continuous monitoring in the diagnosis of landslide mechanisms.

Keywords: case history; monitoring; seasonality; earthquake-induced displacements; landslide hazard assessment

1. Introduction

It is largely recognized that landslides are one of the most widespread geohazards in Europe, producing significant social and economic impacts, and Italy is the most landslide-prone country, with landslides being the most frequent and broad natural hazard (Herrera et al., 2018) [1]. Even though some cases of fast landslides in clay are reported in the literature (Mainsant et al., 2012 [2]), for Italy, slow active landslides are the main type of slope failure that generally take place in geomorphological contexts, where tectonized clayey deposits outcrop (D'Elia et al., 1998 [3]). As pointed out by Picarelli (2007) [4], this class includes large-scale soil bodies that have experienced a general failure, in the sense discussed by Urcioli et al. (2007) [5], and are still moving. Movement is a result of displacements along one or more internal discontinuities, that is, slip surface(s), generated by shear strain localization over which the soil mass slides. According to the classification proposed by Cruden & Varnes (1996) [6], such landslides can be classified as slow, very slow, and extremely slow according to the average rate of movement, typically ranging from a few millimeters to some decimeters per year. A slow rate of movement is often assumed to be uniform with time, and thus creep is considered to be the cause of movement. Although in some cases, viscous-type behaviour of the materials can play some role, good quality displacement measures (Cascini et al., 2014 [7]) demonstrated that the kinematics of such landslides are intermittent, being characterized by accelerations occurring over very short periods.

In particular, it is well documented that the changes in the displacement rate are connected to the pore-water pressure fluctuations within the slope as a consequence of climate variables (Iverson and Major, 1987 [8]; Iverson, 2000 [9]; Alonso et al., 2003 [10]; Calvello et al., 2008 [11]; Schulz et al., 2009 [12]; Tommasi et al., 2013 [13]; Vassallo et al., 2015 [14], among many others). This allows identifying rainfall as the main triggering or aggravating factor affecting the mobility of slow moving landslides. Moreover, these landslides usually fall in high seismicity areas, and thus ground shaking generated by earthquakes is another triggering factor to be considered. Failure modes of seismic-induced landslides are summarized in seismic inventories (Kefeer, 1984 [15]; Delgado et al., (2011) [16]; Martino et al., 2014 [17]) that distinguish coherent landslides (i.e., landslides that move as a single body), disrupted landslides (i.e., rock falls, rock slides, soil falls, and disrupted soil slopes), and lateral spreads or flows. Because of their nature, disrupted instabilities are typically newly formed landslides, while most of seismic induced coherent landslides are reactivation of existing phenomena. At present, instrumental measurements of seismic-induced displacement are very rare in the scientific literature (Lacroix et al., 2014 [18]; Bontemps et al., 2020 [19]), and most of the documented evidences (Hutchinson & Del Prete, 1985 [20]; Kefeer & Manson, 1998 [21]; Al-Homoud & Tahtamoni, 2000 [22]; Pradel et al., 2005 [23]) deal with post-earthquake landslide displacements that were measured or estimated by surface field evidences visible to the naked eye (i.e., large displacements).

With reference to active landslides in clayey formations, the seasonal accelerations related to rainfall events are generally of low intensity and, consequently, harmful consequences to human lives can be avoided, although serviceability problems to existing facilities can be encountered because of cumulative displacements over several years (Urcioli & Picarelli, 2008 [24], Mansour et al., 2011 [25]). On the contrary, seismic loadings can produce sudden and important accelerations of the unstable mass, leading to severe consequences to both people and existing constructions.

In this paper, subsurface displacement time series of an active landslide named "La Sorbella", located in central Italy, are reported and critically analyzed. Manual inclinometer readings clearly highlighted the presence of a sliding surface with an average rate of movement of about 1 cm/year. Such a monitoring system was enhanced by equipping one casing with in-place inclinometer probes, properly installed in correspondence with the sliding surface. Moreover, in order to remotely handle the data, an automated acquisition-transmission system was set up.

The continuous and accurate monitoring system analyzed turned out to be a precious diagnosis instrument, underlying its great potential within the field of landslide hazard assessment. In particular, the recorded data provided much better insight into the response of the landslide to seismic loadings.

2. Material and Methods

2.1. Case History Description

"La Sorbella" landslide is a deep-seated phenomenon that affects a gentle slope hillside (average inclination equal to 8°) oriented west–northwest, in the municipality of Valfabbrica, a small medieval village located in the Apennines chain area, Central Italy. This landslide has been known for a long time and is indicated in the map 1:100,000 by Guzzetti and Cardinali (1989) [26].

From a geological perspective, the rock basement outcropping in the area (Guerrera et al., 2012 [27]) is the Marnoso-Arenacea Formation (MAF), a Miocene foredeep turbidite succession widespread along the north-central Apennines. Such a formation is characterized by an alternation of arenaceous and pelitic layers, whose ratio varies markedly from one area to another. More detailed information about the main MAF facies in the area can be found in Assefa et al., 2017 [28].

Geomorphological features allow inferring the old origin of the landslide, probably triggered in climatic and topographic conditions different from the current ones.

As shown in Figure 1, the landslide body spans between the elevations of 257 and 354 m on medium sea level (m.s.l.) and presents a length of 550 m and maximum width, at the toe, of 600 m.

The lower part of the landslide presents a fan shape, possibly related to the erosion processes of the body sides and deposition at the toe of slope that are typically observed on old landslides.

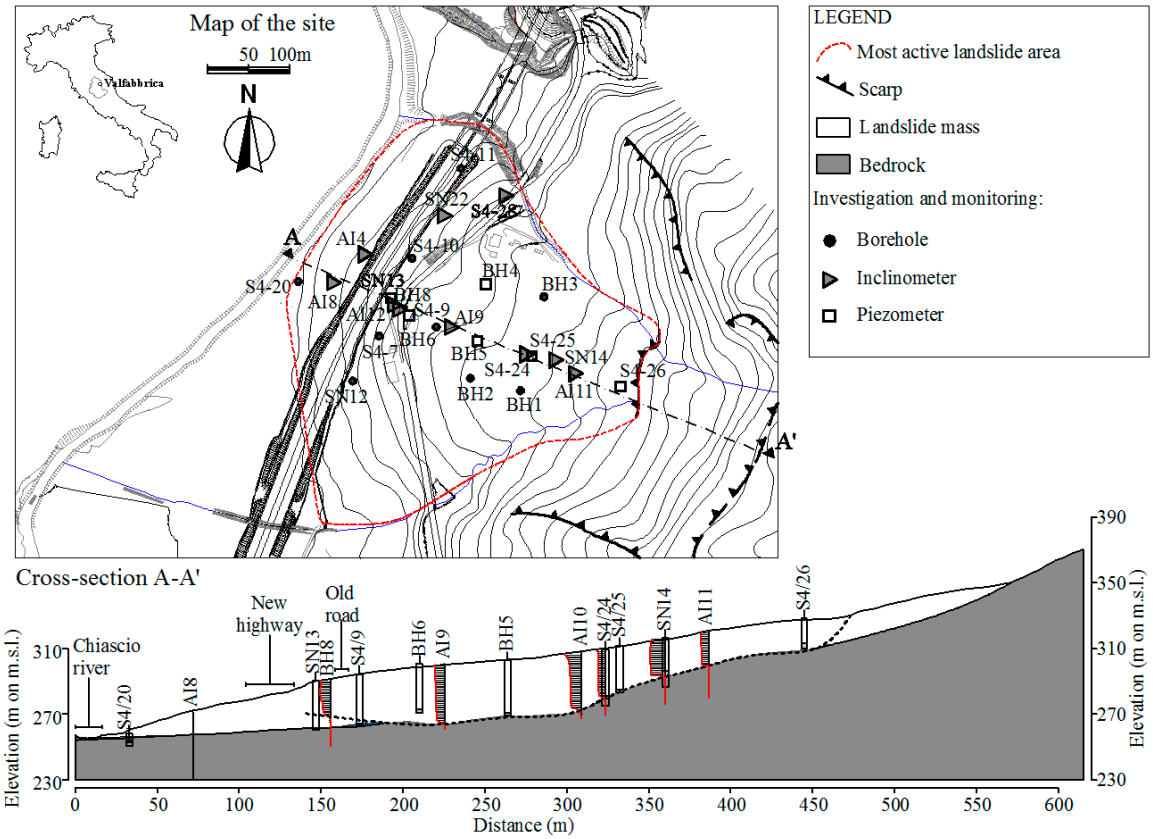

Figure 1. Plan view of the landslide with a longitudinal representative cross section A-A' along the slope.

As shown in the cross section A-A' of Figure 1, geotechnical monitoring based on inclinometer readings allows to define the most active landslide body. This representation shows that the thickness of the landslide body has a maximum value of about 35 m in the center and tapes towards the edges.

In the lower portion of the landslide, an alluvial layer was identified between the basal part of the landslide and the underlying bedrock, demonstrating the large displacements accumulated over the time as the consequence of the instability process.

Geotechnical characterization was based on laboratory testing on undisturbed samples taken from the landslide body. Heterogeneity of the soil samples imposed a careful assessment of result representativeness. The analysis of the particle size distribution indicates the prevalence of the fine fraction, that is, 70–90% of silt and clay. Atterberg limits, according to Casagrande plasticity chart, allow classifying the samples as CL (clay of low plasticity) and ML (silt of low plasticity). A Mohr–Coulomb failure envelope was obtained with negligible effective cohesion and a friction angle between 28° and 32°. Few samples showed higher strength parameters, reflecting the occasional occurrence of coarser grading. The residual shear strength was estimated by shear tests, both direct and ring shear. A failure envelope with a negligible effective cohesion and a friction angle ranging from 14° to 18° was found at the residual. Specific tests on samples taken close to the sliding surface of the landslide are unfortunately missing.

The groundwater level, according to some piezometer measurements, is typically close to the ground surface, with seasonal oscillations from 2 m to 6 m below the surface. In the lower part of the landslide, the presence of the alluvial layer below the sliding mass probably influences the hydraulics of the subsoil.

The old origin of the landslide and the clayey nature of the soil indicate that the movement occurred on an already fully developed sliding surface, where residual strength is largely attained.

This last hypothesis was confirmed by the presence of slickensided discontinuities on the soil coring close to the failure surface. Slickensided discontinuities in clays are typical evidence of the shear zone when experiencing large displacements, and have been observed in other studies on deep-seated landslides in complex clayey formations (Scarpelli et al., 2013 [29]; Segato et al., 2015 [30]; Ruggeri et al., 2016 [31]; Ruggeri et al., 2020 [32]; Ruggeri et al., 2020 [33]). It is interesting to observe that, in several case studies, even the presence of a significant granular fraction could not avoid the reaching of residual conditions along the sliding surface when matrix sustained conditions hold, as documented in Ruggeri et al., 2016 [34].

2.2. Rainfall Regime of the Area

With the aim of investigating the rainfall regime of the area, rainfalls covering the same period of the inclinometer monitoring (2014–2018) were considered. Data, made available by the Servizio Idrografico of Umbria Region (www.annali.regione.umbria.it), come from the Casanuova dam weather station. As this station is located approximately 2 km away from the slope and at the same elevation above sea level (335 m a.s.l.), the recorded data can be considered representative for the investigated site. Daily rainfalls and yearly cumulative rainfalls are shown in Figure 2.

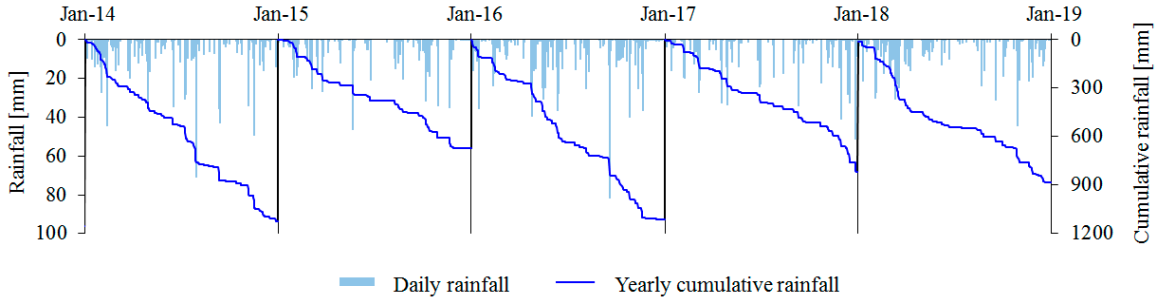

Figure 2. Rainfall regime of the area of interest in the period 2014–2018.

Within the considered period, an annual amount range from 729 mm to 1122 mm was recorded with rainfall distribution, which is typical for the Mediterranean areas. In particular, prolonged rainy days are encountered from the late fall to the end of spring, while the meteoric intake is scarce for the rest of the year, although isolated rainfall events of high intensity sometimes take place during summer.

2.3. Seismic Data

Since August 2016, central Italy has been affected by a long-lasting seismic sequence, with more than 26,000 earthquakes detected by the National Accelerometric Network (RAN) during the first four months, along a 60 km Apennine fault system.

The area of interest is located about 50 km northwest from the epicentral area of the 2016 seismic sequence, characterized by three mainshocks occurring on 24 August (moment magnitude Mw6.0 at Accumoli), 26 October (Mw5.9 at Visso), and 30 October (Mw6.5 at Norcia).

Precisely, "La Sorbella" landslide is situated at 65 km from Accumoli, 45 km from Visso, and 50 km from Norcia. Figure 3a shows the map of central Italy with indication of the epicenters of sequence events with $M_L > 3.5$ occurring in the period August–December 2016 (data taken from http://ran.protezionecivile.it) and at the location of the site of interest. The latter, as demonstrated in Cheloni et al. (2017) [35] using InSAR and GPS data, is located outside the region of significant coseismic displacements.

Thanks to the presence of a seismic station located close to "La Sorbella" landslide (less than 1 km), it was possible to know the actual shaking motion of the area as a consequence of the three mainshocks. In Figure 3b, the position of the Valfabbrica seismic station (VAL) with respect to the landslide is shown together with the main information of the installation site. As reported in the Italian

Accelerometric Archive (http://itaca.mi.ingv.it), the station is installed in a building basement on soil type B (according to the Eurocode 8 classification), evaluated on the basis of geological evidence. Given the small distance between the station and the landslide and the fact that both sites are characterized by similar topographic conditions and outcropping lithotypes, the signals recorded at the VAL station can be considered, as a first approximation, representative of the seismic motions experienced by the landslide.

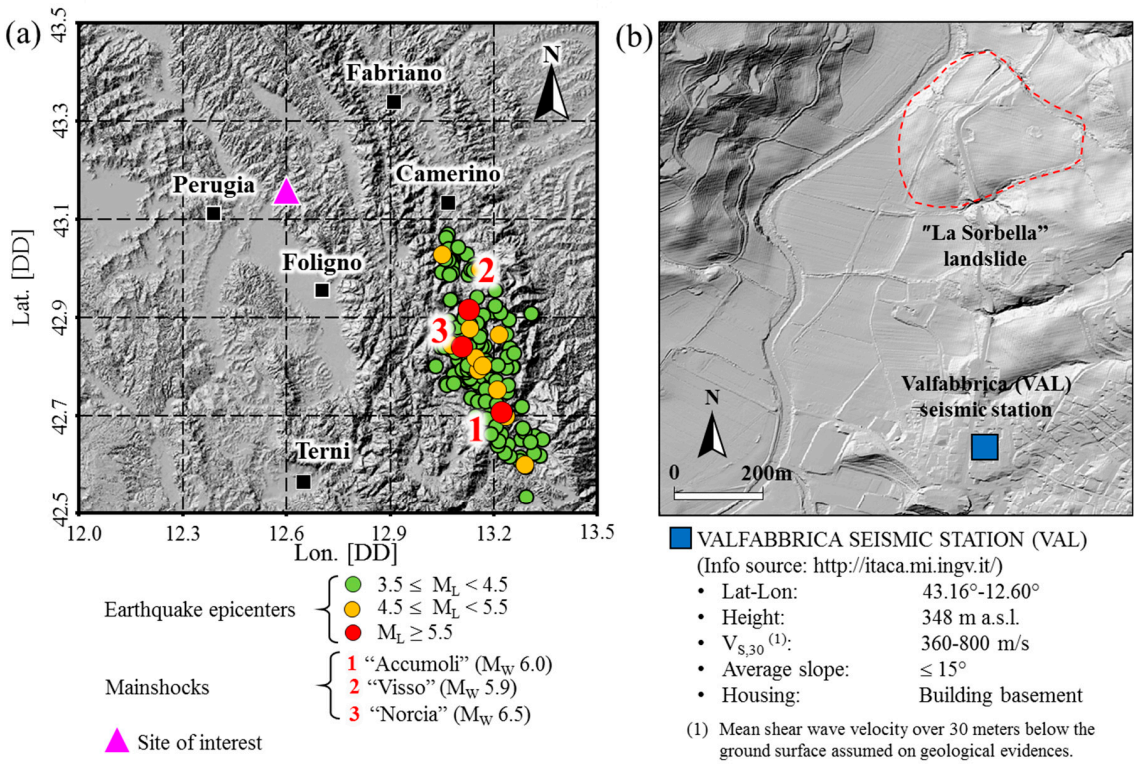

Figure 3. (**a**) Map of central Italy with position of the "Sorbella" landslide and indication of epicenters of seismic events with $M_L > 3.5$ occurring in the period August–November 2016; (**b**) zoom of the site of interest with indication of the landslide and of the closest accelerometric station of "Valfabbrica" (Digital Terrain Model from "Ministero dell'Ambiente e della Tutela del Territorio e del Mare").

Table 1 shows the broad characteristics of the three mainshocks and the main features of the seismic signals recorded at the "Valfabbrica" station (detailed information is available on the website of Italian Department of Civil Protection, National Strong Motion Network-RAN). It can be noted that the peak accelerations experienced in the area of the landslide range from 0.04 g to 0.07 g, that is, rather small when compared with epicentral peak accelerations of higher than 0.8 g (Meletti et al., 2016 [36]).

Table 1. Characteristics of the three considered mainshocks and main features of the seismic signal recorded at the "Valfabbrica" station (VAL).

Characteristics of the Earthquakes					Main Features of the Signals Registered by VAL Station						
Earthquake	**Date**	**hh/mm/ss (UTC)**	**M_W**	**d [Km] ***	**E_d [Km]**	**PGA_E [g]**	**PGA_W [g]**	**PGA_N [g]**	**PGA_S [g]**	**PGA_U [g]**	**PGA_D [g]**
Accumoli	2016-08-24	01:36:32	6.0	8.1	71.5	0.04	0.06	0.03	0.04	0.01	0.01
Visso	2016-10-26	19:18:05	5.9	7.5	50.7	0.04	0.04	0.04	0.04	0.03	0.03
Norcia	2016-10-30	06:40:17	6.5	9.2	54.6	0.07	0.07	0.07	0.06	0.03	0.03

data taken from http://terremoti.ingv.it/ and http://ran.protezionecivile.it
Epicentral distance * Depth PGA_X: Peak ground acceleration directed towards "X" direction

In Figure 4, the acceleration time histories recorded in the east–west, north–south, and up–down directions at the VAL seismic station are plotted. Note that the peak acceleration does not differ significantly from the E–W and N–S components, as the events do not show a relevant directivity.

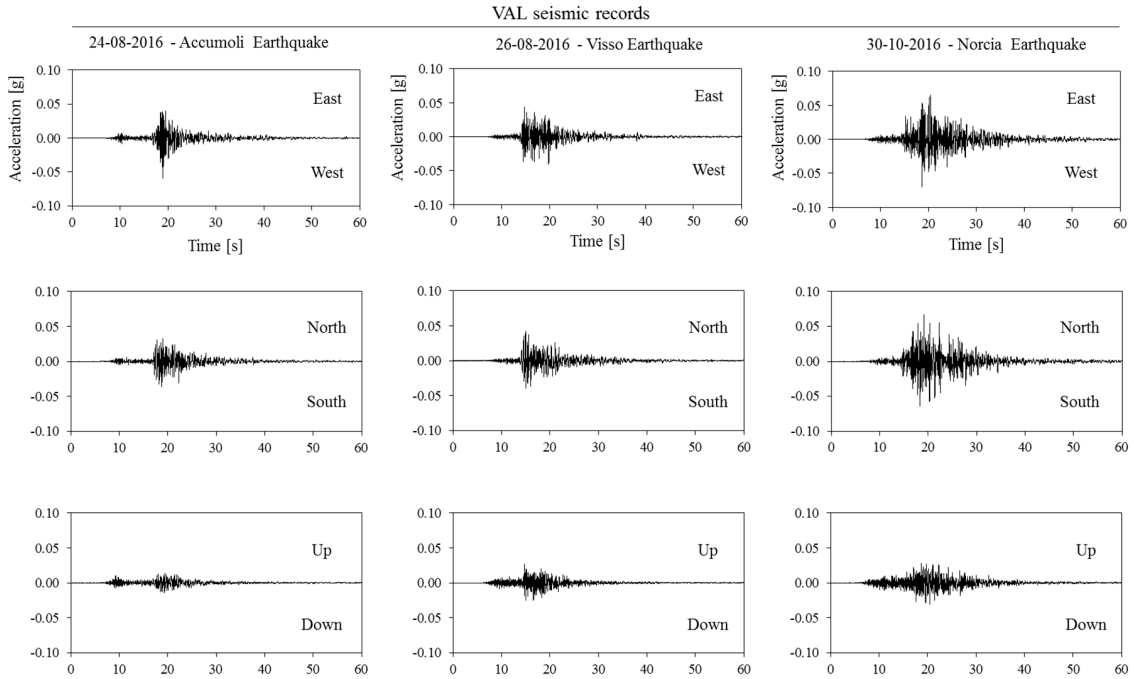

Figure 4. East–west, north–south, and up–down seismic signals recorded at the "Valfabbrica" seismic station (VAL) during the three strong motion events of the 2016 Central Italy seismic sequence.

2.4. Inclinometer Monitoring Systems

In the field of geotechnical monitoring, the inclinometer is a fundamental tool for assessing the landslides' movement. As accurately described by Green and Mikkelsen (1988) [37], it consists of a probe, containing a gravity-actuated transducer (i.e., accelerometer), which is fitted with wheels and lowered by an electrical wire down a grooved casing to control orientation. The wire is connected to a readout unit and data can be recorded manually or automatically. The casing is normally set in vertical drilling holes in such a way to ensure that its movement coincides with that of the ground around it.

Two types of accelerometers are now being used in inclinometer probes: the servo-accelerometer and the micro-electro-mechanical systems (MEMS) accelerometer. The first one, commercially available since 1969, has the highest resolution among the available inclinometers on the market. The MEMS technology derives its name from the MEMS sensors (i.e., micro-electro-mechanical systems), which are a type of process technology used to create tiny integrated devices that combine both mechanical and electrical components. MEMS have been used in inclinometer applications since 2005. They are low power-consuming, durable, and have low costs. Details can be found in the circular n. E-C129 of the Transportation Research Board (USA).

2.4.1. Manual Inclinometer System

Regarding the manual inclinometer system, the probe is moved along the casing at fixed intervals (typically 0.5 or 1.0 m), and its inclination is recorded. By integrating each measure along the vertical, it is possible to determine the profile of the entire casing. The comparison among profiles taken at different dates permits detecting the deformation of the casing over time, which is assumed to be representative of the deformation of the landslide body along the installation axis. In this study, the inclinometer probe used for the manual readings is of servo-accelerometer type, 0.5 m long, with a measuring range of ±30° from the vertical direction and nominal accuracy of ±0.07% FS (full scale).

According to the calibration report, the sensitivity and the accuracy of the device result equal ±0.0004° and ±0.026% FS, respectively. As the readings are typically interpreted in terms of displacements, measures can be affected by a maximum error of ±0.13 mm/m.

2.4.2. Automatic Inclinometer System

To enhance the monitoring system of the landslide, in December 2015, four in-place inclinometer probes were installed within an existing casing in order to continuously monitor the phenomenon. The adopted in-place inclinometer probes are of MEMS type, 1.0 m long, with a measuring range of ±10° from the vertical direction. According to the calibration report, the sensitivity is ±0.0004°, while the accuracy of the device is better than ±0.045% FS. In this case, therefore, measures can be affected by a maximum error equal to ±0.08 mm/m.

To keep the costs of the equipment sufficiently low, the probes were placed at relevant depths only, that is, where the casing profile (as obtained by manual inclinometer system) showed the localization of deformations. It is worth noting that, because of the very slow velocity of the landslide, a daily reading was considered appropriate to properly detect the evolution of the phenomenon.

It is clear that the local measurements of the deformation alone cannot assure the full definition of the vertical displacement profile of the landslide body. So, the readings of the in-place probes were compared with manual ones along the entire depth. This comparison guarantees the representativeness of the local measurements in defining the actual deformation of the sliding mass.

3. Results

3.1. Data of the Manual Inclinometer System

The displacement profiles detected in different periods are shown in Figure 5. The figure clearly shows that the soil mass is sliding on a well-defined shear zone, whose depth ranges between 20 m and 36 m, depending on the considered vertical.

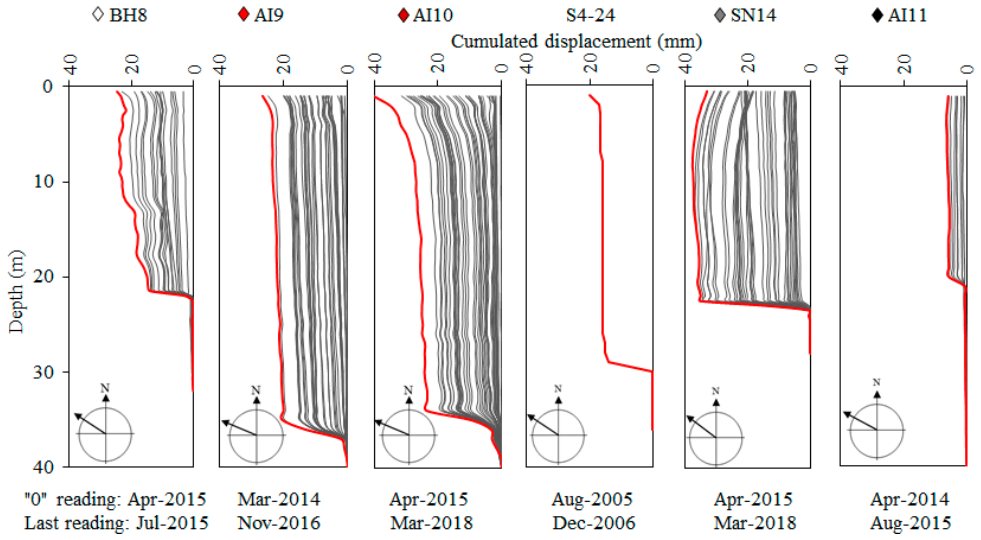

Figure 5. Historical inclinometer profiles obtained by manual readings (each grey line represents a reading of the inclinometer casing taken during the period indicated below the graph; the red line, instead, represents the most recent reading).

On the whole, the unstable volume exhibits a displacement profile with only little internal deformations, as demonstrated by the inclinometer profiles that remain, above the shear zone, mainly vertical as the sliding proceeds.

The presence of a shear zone of limited thickness (thickness lower than 1 m), where almost the entire deformation takes place, allowed to minimize the number of fixed-in-place probes, keeping the significance of the measurements for inferring the displacement of the entire landslide body.

3.2. Data of the Automatic Inclinometer System

In Figure 6a, the evolution of the cumulated displacements of the four in-place AI11 probes from December 2015 to December 2018 is summarized. On the basis of the inclinometer profile obtained by manual readings, the probes were placed at the following relevant depths: Probe 2 (20 m depth) and Probe 3 (22 m) across the identified sliding surface; Probe 1 (4 m) to monitor the soil close to the ground level; and Probe 4 (38 m) to verify that the underlying formation was stable. It can be observed that, after three years of readings, Probe 2 and Probe 3 reached an absolute value of cumulated displacement equal to 48 mm and 20 mm, respectively. On the contrary, Probe 1 and Probe 4 did not exhibit any significant displacement. Daily readings of Probes 2 and 3 demonstrated that the displacement of the landslide was not uniform in time, but exhibited evident accelerations and decelerations, with periods of total statis, with no displacements. Moreover, trends for Probes 2 and 3 were very similar, with the exception of the magnitude of the displacement, which was bigger for Probe 2. However, surprisingly, as demonstrated by the polar plot of the cumulative displacements of Figure 6a, Probes 2 and 3 exhibit displacements with opposite directions; that is, Probe 2 moves downhill, as expected, while Probe 3 moves uphill.

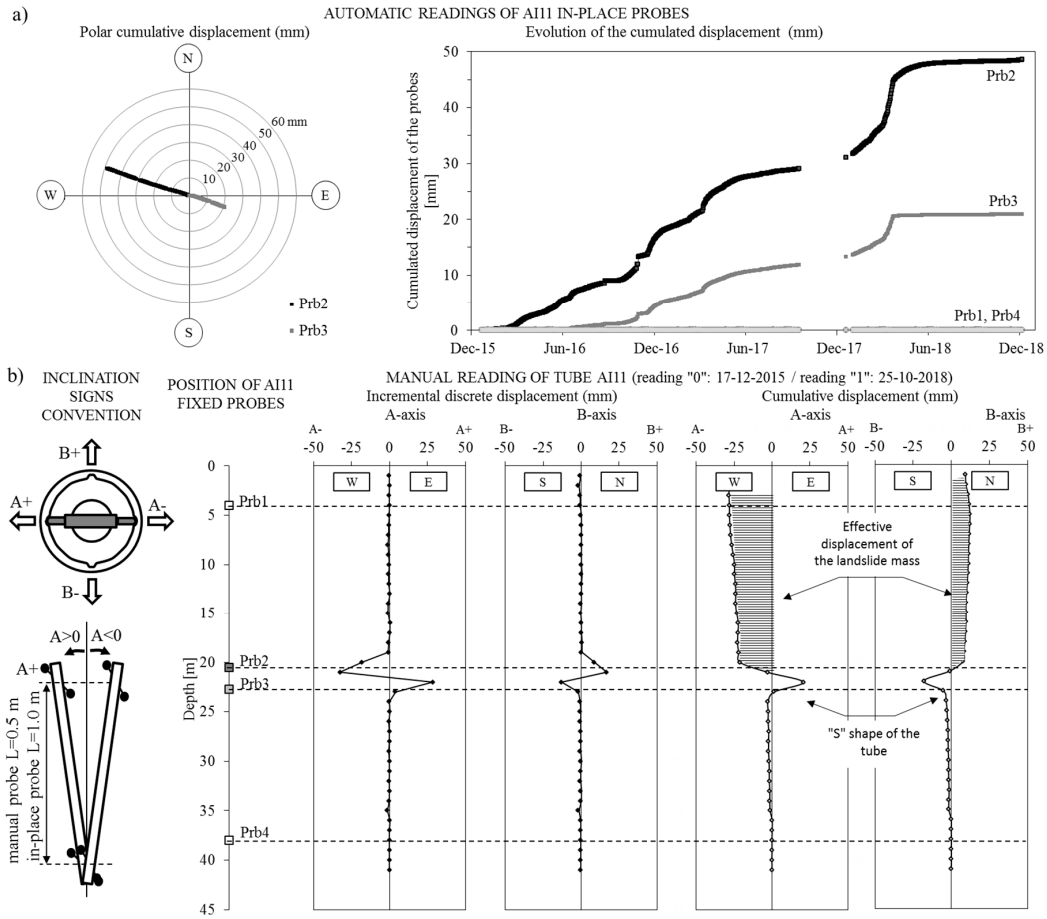

Figure 6. (**a**) Automatic readings of A11 with in-place probes: polar cumulative displacements and evolution in time of the cumulated displacements; (**b**) inclination signs convention of the inclinometer probe, position of the in-place probes along the AI11 casing and results of the manual reading of tube AI11.

To verify the actual functionality of the monitoring system, traditional manual readings were taken in October 2018, after the removal of the in-place probes. Thanks to the availability of the zero reading of the casing (December 2015), the local and the cumulated differential displacement of the entire AI11 inclinometer was obtained, as shown in Figure 6b. It is worth to note that, at the level of the sliding surface (20–22 m depth), the inclinometer guide exhibits a "S" shaped deformation, such that the lower part moves upwards and the upper part downwards. Consequently, the real magnitude of the displacement of the soil mass is the difference between the absolute reading of Probe 2 and the absolute reading of Probe 3.

Beyond these technical difficulties, the evolution of the cumulative displacement resulting after the correction of the AI11 inclinometer readings as well as the corrected daily displacement of the landslide are shown in Figure 7. From now on, this particular plot will be considered the corrected displacement plot, representative of the landslide movement. It can be observed that the displacement of the landslide over the entire period of monitoring is equal to 28 mm.

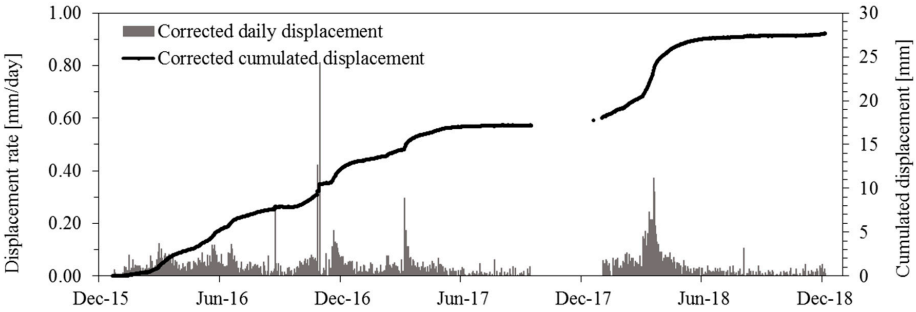

Figure 7. Corrected cumulated displacement and daily displacement from A11 in-place probes.

4. Discussion

The monitoring results are discussed to point out the overall scenario of the landslide resulting from inclinometer measurements and identify the response of the landslide to rainfalls and to earthquake shakings. It is known that seismic motions can affect the hydraulic response of the landslides (Cotecchia, 2006 [38]), but in this study, such a possible influence was not analysed.

4.1. Overall Scenario from Inclinometer Measurements

The landslide has been monitored through inclinometers since 2001, but most of the data have been collected from 2014. Taking into account the type of soil that constitutes the landslide body and the type of deformation exhibited by inclinometer readings (see Figure 5), the phenomenon is an "earth slide" according to the traditional classification of the movement (Varnes, 1978 [39]; Hungr et al., 2014 [40]). The sliding surface appears substantially planar and only small rotation and limited backward tilting occur; this means that, even though the landslide body is constituted by soil, the mechanism of deformation of "La Sorbella" is very similar to that observed in rock for the block slide type of movement. On other terms, the instable mass moves downslope as a relatively coherent mass, without diffuse deformations within the landslide body. This finding is supported by the cumulative displacement trends for most representative inclinometer logs that are represented in Figure 8. In fact, the general agreement among the different readings means the landslide moves substantially as a unique body, with average displacement rates between 10 and 15 mm/year. According to Cruden and Varnes [6], with such rates, it is possible to classify the landslide as an extremely slow phenomenon, and considering the classification adopted by seismic inventories, this finding allows to define "La Sorbella" as a coherent landslide.

In Figure 8, the daily readings from in-place probes at the vertical AI11, available since December 2015, are also reported. The coherence in time is evident between the manual and automatic readings for vertical AI11, supporting the reliability of the unusual deformation of the inclinometer casing

pointed out by the readings of Probes 2 and 3. A possible explanation for a similar casing deformation could be a significant vertical stress component induced by the landslide on the casing itself. A similar phenomenon has been observed by Jeng et al., 2017 [41].

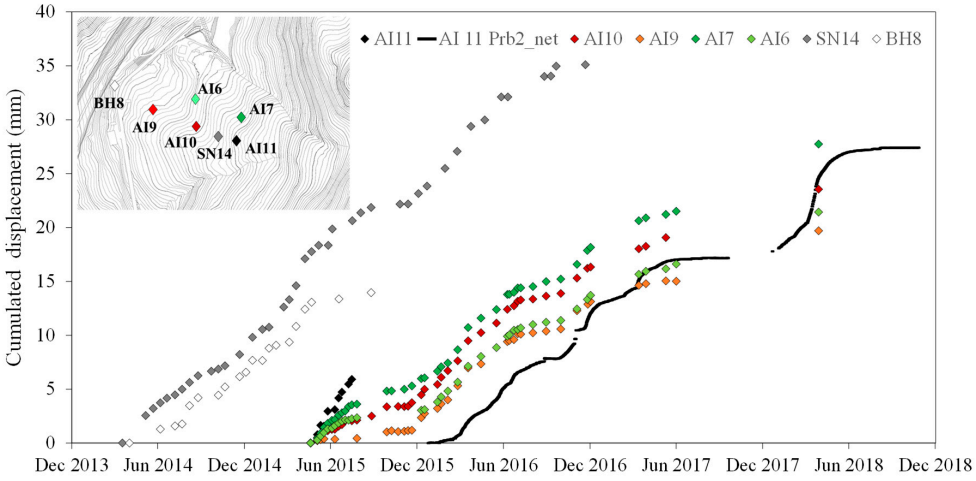

Figure 8. Cumulative displacement obtained by means of manual and in-place probes from 2014. The continuous graph represents the corrected cumulated displacement from in-place probes.

4.2. Rainfall-Induced Displacements

It is relevant to point out the pattern of rainfall-induced displacements to establish a reference interpretation of the physics of the landslide. To this aim, in Figure 9, three different episodes of displacements are selected and analyzed. For each episode, the daily and cumulative rainfalls are compared with the daily and cumulative displacements. After the activation, the displacement rate remains high for several days, even without any intake (see episodes 1 and 2 of Figure 9), so that the decrease of the displacement rate takes place progressively. Moreover, the data indicate that the maximum velocity induced by rainfalls is always less than 0.4 mm/day.

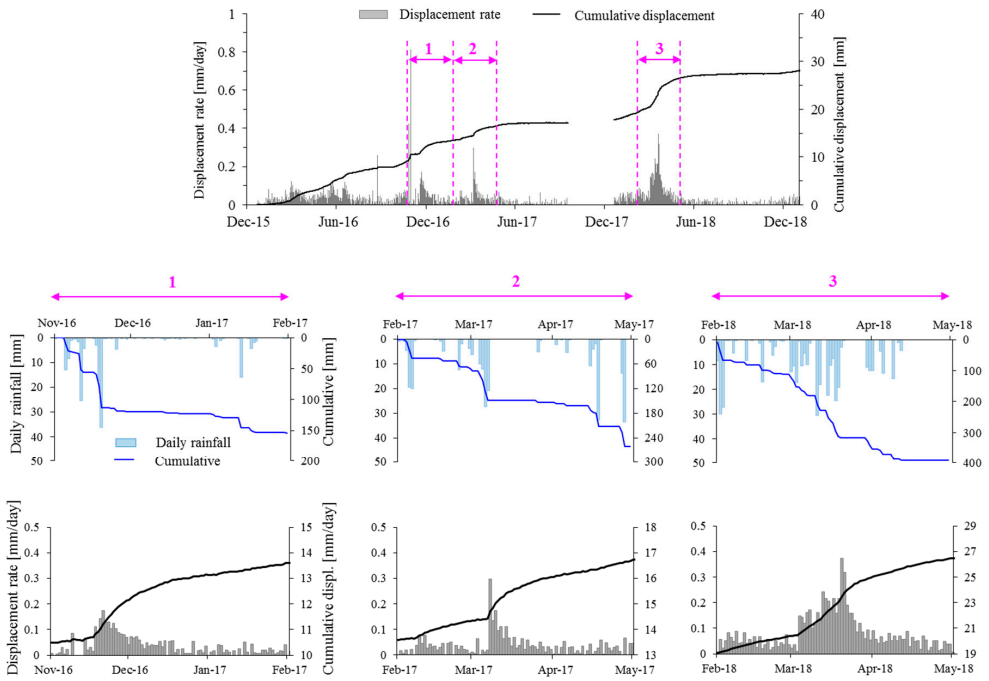

Figure 9. Focus on three reactivations of the landslide movement originated by rainfall: comparison between daily and cumulated rainfalls versus daily and cumulative displacements for AI11.

In conclusion, the daily readings of the inclinometers pointed out the intermittent kinematics of the landslide, proving a clear connection between the displacement rate and the rainfall regime. These observations tend to exclude creep as the cause of the movement for slow active landslides, as stated by Picarelli (2007) [4].

4.3. Seismic-Induced Displacements

A careful analysis of the daily readings of the AI11 in-place inclinometer probes highlighted some clear signs of movement not related to rainfall events. In particular, three well-defined spikes of daily displacements were recorded exactly in the days of the three mainshocks of the 2016 seismic sequence (see Figure 10). Precisely, the displacements exhibited by the landslide were equal to 0.3 mm, 0.4 mm, and 0.8 mm on 24 August, 26 October, and 30 October, respectively. The relevance of the three peaks that cannot be confused with other values of displacements recorded in the period of interest is evident: all three peaks are of the same order or higher than the maximum value of daily displacements exhibited after heavy rainfalls. Moreover, the simultaneous occurrence of the displacements with the three main shocks justifies the link between the seismic shaking episodes and observed response of the landslide, thus giving the very rare opportunity to collect field data on seismic-induced displacement for an active landslide. This new result updates the preliminary analysis presented in Ferretti et al. (2019) [42].

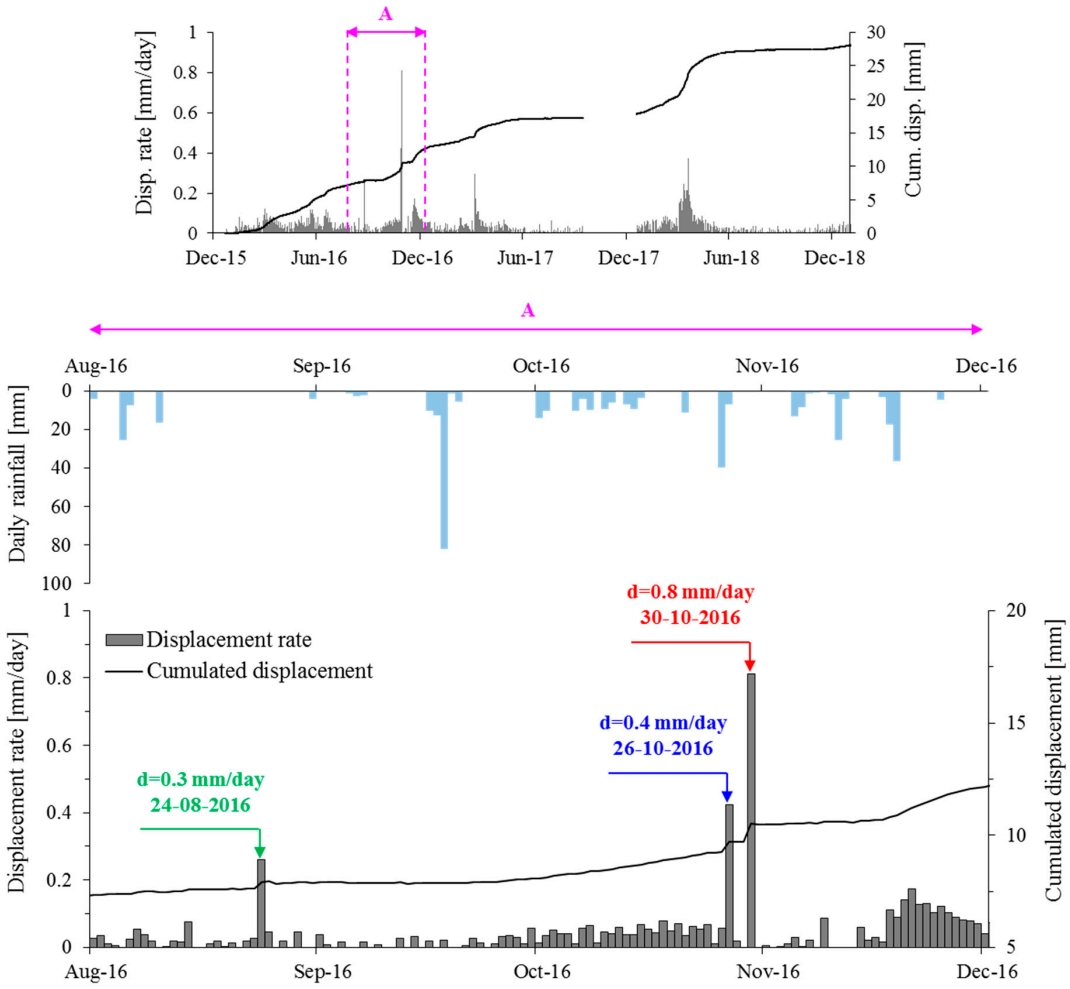

Figure 10. Daily and cumulated displacement from AI11 in-place inclinometer probes with a focus on the period of the three strong earthquake events of the seismic sequence; daily rainfalls are reported for the same period.

The availability of daily readings of displacements allows an interesting observation about the effect of an earthquake on the landslide. Different from what was observed for rainfall-induced displacements, the landslide response to the earthquake is immediate and without delayed effects after the triggering, that is, the end of the seismic excitation corresponds to the end of the seismic-displacements. In contrast, Lacroix et al. (2014) [18] report a case study where a landslide suffered clear coseismic displacements, but exhibited a postseismic motion for weeks, with a cumulative displacement three times greater than the coseismic one. The same authors cite case histories where the activation took place only after the earthquake. The behaviour of "La Sorbella" is very likely the consequence of the specific stress state at the sliding surface of an active landslide in clayey soil: soil strength at residual with a perfectly plastic rheology, without strain-softening or excess pore pressures induced by the sliding. On other terms, the sliding process of a landslide on a mature failure surface in clay is mainly developed at a constant volume, with no induced changes in the pore water pressure nor decreasing in shear strength. This statement finds a strong experimental confirmation when compared with the results of direct shear tests at the residual: when the shearing takes place on a fully developed failure surface, one observes no volume changes, no pore water pressure increase, and no decrease of shear strength.

The long-lasting seismic sequence offered many aftershock events that did not induce any clear displacement on the landslide. Even though the peak ground acceleration (PGA) is not the only parameter controlling the landslide displacement, it appears events with peak acceleration lower than 0.010–0.013 g at the Valfabbrica seismic station were not able to activate the landslide.

Estimation of Critical Acceleration from Measured Data

Two aspects of the seismic response of the "La Sorbella" landslide are discussed here: the distance of the landslide from the earthquakes epicenters and the critical acceleration exhibited by an active landslide.

Seismic induced landslides are typically observed close to the epicenters of the seismic events, even if some failures triggered by faraway earthquakes are reported in the scientific literature. Keefer (1984) [15] and Delgado et al. (2011) [16], processing a comprehensive inventory of earthquakes, proposed an empirical relationship to represent an upper bound limit of the distance from observed seismic induced landslide and magnitude (or intensity) of earthquakes. Referring to coherent landslides, Figure 11 shows that, according to the observations reported in the literature, the three considered mainshocks were able to induce landslide up to 50–80 km from the epicenters. "La Sorbella" landslide is located close to the upper bound distance at which seismic-induced effects are expected. This fact appears consistent with the millimetric movements observed for the considered landslide, so that the registered data seem to confirm the soundness of the upper limit proposed by Delgado for the appearance of large seismic-induced movements. Moreover, present observations on "La Sorbella" landslide phenomenon fully confirm Delgado's observations on the sensitivity of landslides in marly clay formations to the effects of far field earthquakes.

A second aspect of interest is the evaluation of the critical acceleration of the landslide, considering that "La Sorbella" was already an active phenomenon interfering with a road infrastructure. It is known that the evaluation of the critical acceleration of a landslide is a relevant issue within the engineering perspective, because it allows to estimate the seismic risk of a given infrastructure. Critical acceleration is defined as the value of acceleration, constant in time and in space, which produces a state of incipient failure. The application of this definition to an already active landslide, that is, a landslide with a safety factor close to 1, makes the estimation of the critical acceleration particularly awkward. Critical acceleration is the fundamental ingredient to apply Newmark's method (Newmark, 1965 [43]; Jibson, 2011 [44]), which is a well-known displacement criterion to evaluate the safety of slopes in seismic conditions. Newmark assumes that permanent displacements take place when the inertial forces induced by an earthquake on a potential sliding mass exceed the resisting forces that result from mobilization of shear strength along the failure surface. By assuming the material above the failure surface as rigid, Newmark showed that the seismic slope stability problem was

analogous to the problem of a rigid block resting on an inclined plane. The block slides only if the earthquake acceleration becomes larger than its critical acceleration. The critical acceleration, a_y, can be evaluated by a limit equilibrium analysis of the system, adding inertial horizontal and vertical accelerations of the block mass to gravity. The displacement of a block under earthquake loading can be evaluated by a double integration of the dynamic equilibrium equation for the time intervals when the earthquake acceleration exceeds the yield acceleration (i.e., the critical acceleration) of the block (see Figure 12a). Although this method was proposed for computing the coseismic displacement of a dam, at present, even considering the improvements proposed by several authors (Makdisi, 1978 [45]; Bray and Travasarou, 2007 [46]), it is widely accepted as an intermediate analysis to fill the gap between the pseudo-static and stress-deformation families of analysis.

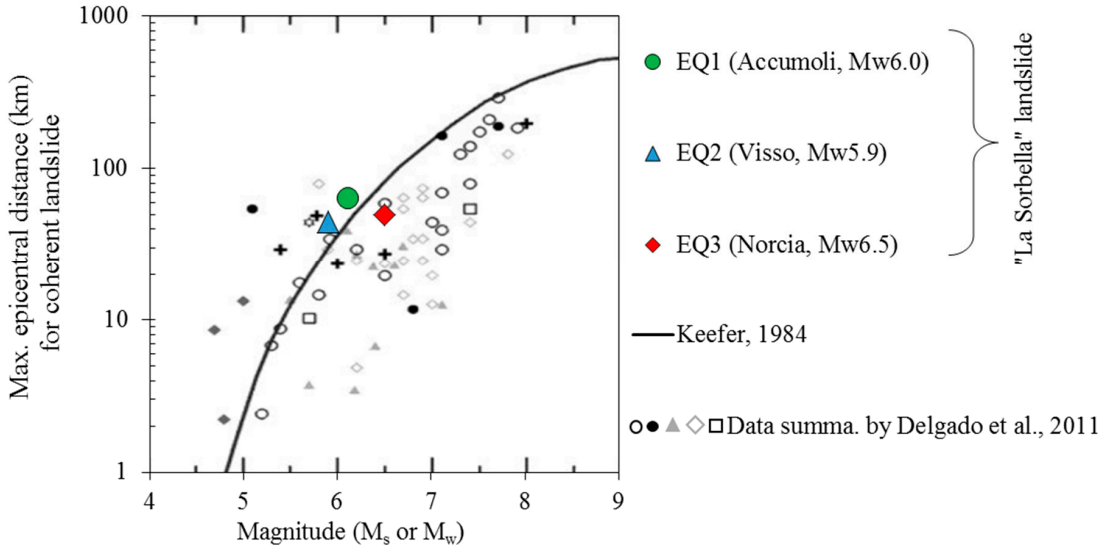

Figure 11. Distribution of maximum distances for seismic-induced landslides as a function of earthquake magnitude: current data versus literature data (modified from Delgado et al, 2011 [16]).

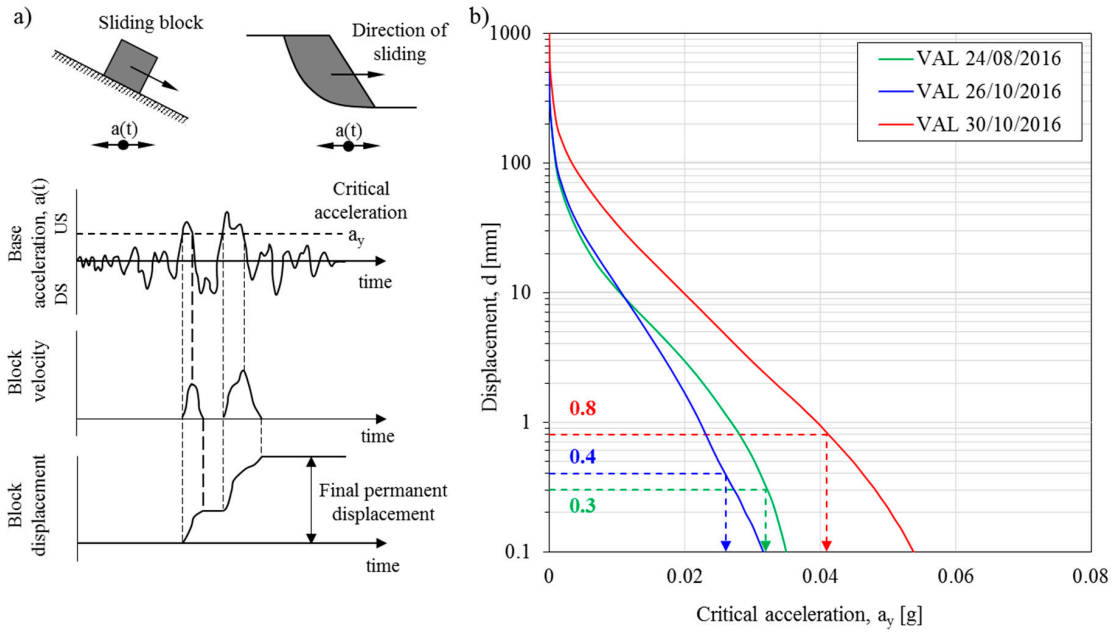

Figure 12. (**a**) Newmark sliding block concept for slopes; (**b**) relationship between permanent displacement (d) and critical acceleration (a_y) for the three selected signals; the arrows show the critical acceleration related to the observed displacement of the landslide.

In the present case study, the availability of measured displacement exhibited by a soil mass caused by three different earthquakes, as well as the corresponding seismic signals recorded at a seismic station close to the triggered landslide, offer a very rare opportunity to estimate, through a back analysis procedure, a credible value of the critical acceleration for the landslide.

Operatively, the E–W acceleration of the three mainshocks recorded at the "Valfabbrica" station, which is oriented approximately in the same direction of the landslide, was double integrated after a basic baseline correction of the seismic signal Tropeano (2010) [47]. In Figure 12b, the relationship between permanent displacement (d) and critical acceleration (a_y) is shown. Now, by referring to the displacement measured in AI11, the critical acceleration of the landslide results equal 0.032 g, 0.026 g, and 0.041 g for the Accumoli, Visso, and Norcia earthquake, respectively. Despite the large number of simplified hypotheses, the observed range of values is in fair agreement with the results of different authors (Crespellani et al., 2003 [48], Pradel et al., 2005 [23]), who estimated an initial critical acceleration ranging from 0.020 g to 0.050 g for the reactivation of large landslides. Moreover, it appears relevant that the critical acceleration of "La Sorbella", where the displacements were very limited, matches very well with the values of literature back-calculated for landslides, where coseismic displacements have been of decades of centimeters. This observation suggests that critical acceleration of pre-existing landslides in clay is scarcely affected by the amount of the displacement induced on the sliding mass. This behavior could be rationally related to the fact that, for active sliding on clayey formation, the residual strength is already attained on the sliding surface, and that displacements on a pre-existing surface are mainly because of a shear, thus excluding large modification of the shear strength as the displacement increases (i.e., no significant pore water pressure development or further reduction of the soil shear strength). As a consequence, it is reasonable to observe very close values of critical acceleration for small and large displacements.

5. Conclusions

The automation of the monitoring of an existing deep-seated landslide, implemented to mitigate the risk of an important highway crossing Italy east–west, allowed to point out the landslide response to different natural forcings, such as rainfall and earthquakes. An existing conventional monitoring system was enhanced by means of in-place inclinometers connected to a mobile network, so that the site measurements were collected and transmitted in real-time to a server. Through the daily readings acquired by the monitoring system, it was possible to obtain a detailed description of the motion characters of the landslide and to understand the main causes governing its mechanics.

With regard to the response to rainfalls, it was possible to observe that the rate of displacement is very low on average, but is not constant in time, being the consequence of single displacement increments related to any single rainfall event. Moreover, after the activation and even without any rainwater intake, the displacement rate remains high for several days, indicating a sort of relaxation process lasting several days.

Concerning the effect of the earthquakes, the in-place inclinometer probes have furnished the profile of the displacements of the landslide owing to the seismic sequence that hit central Italy in 2016. Coseismic landslides are a well-recognized secondary hazard of earthquakes in mountainous and hilly regions, producing large damage to linear infrastructures (i.e., railways, roads, pipelines), with a high impact on the costs of reconstruction. Typically, real observations in this field are particularly rare. The three mainshocks of the long-lasting sequence have all produced permanent displacements along the rupture surface of the sliding mass. These displacements were small, but nevertheless consistent with the low energy shaking motions experienced by the landslide. These data, together with the knowledge of the characteristic of the input motion, have allowed to estimate the critical acceleration (a_y) of the sliding mass from real observations, by means of Newmark's approach.

Apart from the specific value of the critical acceleration obtained by the presented procedure, it is relevant to underline the great potential of continuous monitoring to reduce the risk on infrastructures located in landslide-prone areas.

Author Contributions: Conceptualization, V.M.E.F., P.R.; Data curation, A.F.; Investigation, A.F.; Methodology, V.M.E.F.; Funding acquisition, G.S.; Supervision, G.S.; Writing—original draft, P.R.; Writing—review & editing, P.R., V.M.E.F., A.F. and G.S. All authors have read and agreed to the published version of the manuscript.

Funding: This research was funded by ITALIAN MINISTRY OF UNIVERSITY AND RESEARCH, grant number PRIN201572YTLA_005.

Acknowledgments: Many thanks to Astaldi S.p.A. and DIRPA2 S.c.a.r.l. for the provided data.

Conflicts of Interest: The funders had no role in the design of the study; in the collection, analyses, or interpretation of data; in the writing of the manuscript; or in the decision to publish the results.

References

1. Herrera, G.; Herrera, G.; Mateos, R.M.; García-Davalillo, J.C. Landslide databases in the geological surveys of europe. *Landslides* **2018**, *15*, 359–379. [CrossRef]
2. Mainsant, G.; Larose, E.; Brönnimann, C.; Jongmans, D.; Michoud, C.; Jaboyedoff, M. Ambient seismic noise monitoring of a clay landslide: Toward failure prediction. *J. Geophys. Res.* **2012**, *117*, F01030. [CrossRef]
3. D'Elia, B.; Picarelli, L.; Leroueil, S.; Vaunat, J. Geotechnical characterization of slope movements in structurally complex clay soils and stiff jointed clays. *Riv. Ital. Geotec.* **1998**, *3*, 5–32.
4. Picarelli, L. Considerations about the mechanics of slow active landslides in clay. In *Progress in Landslide Science*; Sassa, K., Fukuoka, H., Wang, F., Wang, G., Eds.; Springer: Berlin, Germany, 2007; pp. 27–57.
5. Urcioli, G.; Picarelli, L.; Leroueil, S. Local soil failure before general slope failure. *Geotech. Geol. Eng.* **2007**, *25*, 103–122. [CrossRef]
6. Cruden, D.M.; Varnes, D.J. Landslide types and processes. In *Landslides: Investigation and Mitigation*; Special Report 247; Transportation Research Board: Washington, DC, USA, 1996; pp. 36–75.
7. Cascini, L.; Calvello, M.; Grimaldi, G.M. Displacement trends of slow-moving landslides: Classification and forecasting. *J. Mater. Sci.* **2014**, *11*, 592–606. [CrossRef]
8. Iverson, R.M.; Major, J.J. Rainfall, groundwater f low, and seasonal motion at minor creek landslide, northwestern California: Physicali nterpretationo f empiricalr elations. *Geol. Soc. Am. Bull.* **1987**, *99*, 579–594. [CrossRef]
9. Iverson, R.M. Landslide triggering by rain infiltration. *Water Resour. Res.* **2000**, *36*, 1897–1910. [CrossRef]
10. Alonso, E.E.; Gens, A.; Delahaye, C.H. Influence of rainfall on the deformation and stability of a slope in overconsolidated clays: A case study. *Hydrogeol. J.* **2003**, *11*, 174–192. [CrossRef]
11. Calvello, M.; Cascini, L.; Sorbino, G. A numerical procedure for predicting rainfall-induced movements of active landslides along pre-existing slip surfaces. *Int. J. Numer. Anal. Methods Geomech.* **2008**, *32*, 327–351. [CrossRef]
12. Schulz, W.H.; McKenna, J.P.; Kibler, J.D. Relations between hydrology and velocity of a continuously moving landslide—Evidence of pore-pressure feedback regulating landslide motion? *Landslides* **2009**, *6*, 181–190. [CrossRef]
13. Tommasi, P.; Boldini, D.; Caldarini, G.; Coli, N. Influence of infiltration on the periodic re-activation in an overconsolidated clay slope. *Can. Geotech. J.* **2013**, *50*, 54–67. [CrossRef]
14. Vassallo, R.; Grimaldi, G.M.; Di Maio, C. Pore water pressures induced by historical rain series in a clayey landslide: 3D modelling. *Landslides* **2015**, *12*, 731–744. [CrossRef]
15. Keefer, D.K. Landslides caused by earthquakes. *Geol. Soc. Am. Bull.* **1984**, *95*, 406–421. [CrossRef]
16. Delgado, J.; Garrido, J.; López-Casado, C.; Martino, S.; Peláez, J.A. On far field occurrence of seismically induced landslides. *Eng. Geol.* **2011**, *123*, 204–213. [CrossRef]
17. Martino, S.; Prestininza, A.; Romeo, R.W. Earthquake-induced ground failures in Italy from a reviewed database. *Nat. Hazards Earth Syst. Sci.* **2014**, *14*, 799–814. [CrossRef]
18. Lacroix, P.; Perfettini, H.; Taipe, E.; Guillier, B. Co-and Postseismic motion of a landslide: Observations, modelling and analogy with tectonic faults. *Geophys. Res. Lett.* **2014**, *41*, 6676–6680. [CrossRef]
19. Bontemps, N.; Lacroix, P.; Larose, E.; Jara, J.; Taipe, E. Rain and small earthquakes maintain a slow-moving landslide in a persistent critical state. *Nat. Commun.* **2020**, *11*. [CrossRef] [PubMed]
20. Hutchinson, J.N.; Del Prete, M. Landslide at Calitri, southern Apennines, reactivated by the earthquake of 23rd November 1980. *Geol. Appl. Idrogeol.* **1985**, *20*, 9–38.

21. Kefeer, D.K.; Manson, M.W. Regional distribution and characteristics of landslides generated by the earthquake. In *The Loma Prieta, California, Earthquake of October 17, 1989-Landslides*; U.S. Geological Survey Professional Paper 1551-C; Kefeer, D.K., Ed.; U.S. Geological Survey: Reston, VA, USA, 1998; pp. 7–32.
22. Al-Homoud, A.S.; Tahtamoni, W. Comparison between predictions using different simplified Newmark's block-on-plane models and field values of earthquake induced displacements. *Soil Dyn. Earthq. Eng.* **2000**, *19*, 73–90. [CrossRef]
23. Pradel, D.E.; Smith, P.M.; Stewart, J.P.; Raad, G. Case history of landslide movement during the Northridge earthquake. *J. Geotech. Geoenviron. Eng.* **2005**, *131*, 1360–1369. [CrossRef]
24. Urcioli, G.; Picarelli, L. Interaction between landslides and man-made works. In *Landslides and Engineered Slopes—From the Past to the Future, Proceedings of the 10th International Symposium on Landslides and Engineered Slopes, Xi'an, China, 30 June–4 July 2008*; Chen, Z., Zhang, J., Li, Z., Wu, F., Ho, K., Eds.; CRC Press: Boca Raton, FL, USA, 2008; Volume 2, pp. 1301–1307.
25. Mansour, M.F.; Morgenstern, N.R.; Martin, C.D. Expected damage from displacement of slow-moving slides. *Landslides* **2011**, *8*, 117–131. [CrossRef]
26. Guzzetti, F.; Cardinali, M. Carta Inventario dei fenomeni franosi della regione dell'umbria ed aree limitrofe. *CNR GNDCI* **1989**, *204*, 2.
27. Guerrera, F.; Tramontana, M.; Donatelli, U. Space/time tectono-sedimentary evolution of the Umbria Romagna-Marche Miocene Basin (North Apennines, Italy). *Swiss J. Geosci.* **2012**, *105*, 325–341. [CrossRef]
28. Assefa, S.; Graziani, A.; Lembo-Fazio, A. A slope movement in a complex rock formation: Deformation measurements and DEM modelling. *Eng. Geol.* **2017**, *219*, 74–91. [CrossRef]
29. Scarpelli, G.; Segato, D.; Sakellariadi, E.; Vita, A.; Ruggeri, P.; Fruzzetti, V.M.E. Slope instability problems in Jonica highway construction. In *Landslide Science and Practice: Risk Assessment*; Springer: Berlin, Germany, 2013; pp. 275–282.
30. Segato, D.; Scarpelli, G.; Fruzzetti, V.M.E.; Ruggeri, P.; Vita, A.; Paternesi, A. Excavation works in stiff jointed clay material: Examples from the trubi formation, southern Italy. *Landslides* **2015**, *12*, 721–730. [CrossRef]
31. Ruggeri, P.; Fruzzetti, V.M.E.; Vita, A.; Paternesi, A.; Scarpelli, G.; Segato, D. Deep-seated landslide triggered by tunnel excavation. In *Landslides and Engineered Slopes, Experience, Theory and Practice*; CRC Press: Boca Raton, FL, USA, 2016; Volume 3, pp. 1759–1766.
32. Ruggeri, P.; Fruzzetti, V.M.E.; Scarpelli, G. Lessons Learnt from the SS 106 Jonica Highway Construction Works. *Lect. Notes Civ. Eng.* **2020**, *40*, 734–742.
33. Ruggeri, P.; Fruzzetti, V.M.E.; Scarpelli, G. Design Strategies to Mitigate Slope Instabilities in Structurally Complex Formations. *Geosciences* **2020**, *10*, 82. [CrossRef]
34. Ruggeri, P.; Segato, D.; Fruzzetti, V.M.E.; Scarpelli, G. Evaluating the shear strength of a natural heterogeneous soil using reconstituted mixtures. *Géotechnique* **2016**, *66*, 941–946. [CrossRef]
35. Cheloni, D.; De Novellis, V.; Albano, M.; Antonioli, A.; Anzidei, M.; Atzori, S.; Avallone, A.; Bignami, C.; Bonano, M.; Calcaterra, S. Geodetic model of the 2016 central italy earthquake sequence inferred from insar and GPS data. *Geophys. Res. Lett.* **2017**, *44*, 6778–6787. [CrossRef]
36. Meletti, C.; Visini, F.; D'Amico, V.; Rovida, A. Seismic hazard in central Italy and the 2016 Amatrice earthquake. *Ann. Geophys.* **2016**, *59*. [CrossRef]
37. Green, G.E.; Mikkelsen, P.E. Deformation measurements with inclinometers. In *Transportation Research Record 1169, TRB*; National Research: Council, China, 1988; pp. 1–15.
38. Cotecchia, V. Experience drawn from the great Ancona landslide of 1982. The second hans cloos lecture. *Bull. Eng. Geol. Environ.* **2006**, *65*, 1–41. [CrossRef]
39. Varnes, D.J. Slope movement types and processes. In *Landslides, Analysis and Control, Special Report 176: Transportation Research Board*; Schuster, R.L., Krizek, R.J., Eds.; National Academy of Sciences: Washington, DC, USA, 1978; pp. 11–33.
40. Hungr, O.; Leroueil, S.; Picarelli, L. The Varnes classification of landslide types, an update. *Landslides* **2014**, *11*, 167–194. [CrossRef]
41. Jeng, C.-J.; Yo, Y.-Y.; Zhong, K.-L. Interpretation of slope displacement obtained from inclinometers and simulation of calibration tests. *Nat. Hazards* **2017**, *87*, 623–657. [CrossRef]

42. Ferretti, A.; Fruzzetti, V.M.E.; Ruggeri, P.; Scarpelli, G. Seismic induced displacements of "La Sorbella" landslide. In Proceedings of the VII International Conference on Earthquake Geotechnical Engineering, Earthquake Geotechnical Engineering for Protection and Development of Environment and Constructions, Rome, Italy, 17–20 June 2019; pp. 2373–2380.
43. Newmark, N.M. Effects of earthquakes on dams and embankments. *Geotechnique* **1965**, *15*, 139–160. [CrossRef]
44. Jibson, R.W. Methods for assessing the stability of slopes during earthquakes—A retrospective. *Eng. Geol.* **2011**, *122*, 43–50. [CrossRef]
45. Makdisi, F.I.; Seed, H.B. Simplified procedure for estimating dam and embankment earthquake-induced deformations. *ASCE J. Geotech. Eng. Div.* **1978**, *104*, 849–867.
46. Bray, J.D.; Travasarou, T. Simplified procedure for estimating earthquake-induced deviatoric slope displacements. *J. Geotech. Geoenviron. Eng.* **2007**, *133*, 381–392. [CrossRef]
47. Tropeano, G. Previsione di Spostamenti Di Pendii in Condizioni Sismiche. Ph.D. Thesis, University of Calabria, Rende, Italy, 2010.
48. Crespellani, T.; Facciorusso, J.; Madiai, C.; Vannucchi, G. Influence of uncorrected accelerogram processing techniques on Newmark's rigid block displacement evaluation. *Soil Dyn. Earthq. Eng.* **2003**, *23*, 415–424. [CrossRef]